Journal of Advanced Marine Engineering and Technology, Vol. 46, No. 6, pp. 317~325, 2022
J. Advanced Marine Engineering and Technology (JAMET)
https://doi.org/10.5916/jamet.2022.46.6.317

ISSN 2234-7925 (Print)
ISSN 2765-4796 (Online)
Original Paper

Study on the vibration behavior of a G/T 3-ton class composite fishing boat hybrid propulsion system

Quang Dao Vuong[1] · Youngmin Kim[2] · Ji-woong Lee[†]

(Received November 13, 2022 ; Revised December 1, 2022 ; Accepted December 15, 2022)

Abstract: In recent years, eco-friendly ships have been widely used to optimize energy efficiency and prevent air pollution. Composite materials can reduce the weight of vessels, reduce maintenance costs and time, and maximize vessel life. In addition, if a ship is equipped with a hybrid propulsion system, its prime movers can be alternated, improving its flexibility in various maneuvering conditions. However, the vibration behavior of the ship should be confirmed when new materials are used for the ship hull and for new hybrid transmission configurations. In this study, the performance of a hybrid propulsion system for a 3-ton G/T-class composite fishing boat was evaluated through experiments during a sea trial. The results revealed that torsional vibration exhibits resonance in the propeller speed range of 300 to 350 rpm. The level of resonance is not sufficiently high to damage the shaft, but it may cause the electromagnetic clutch to slip. Thus, propeller efficiency is not maximized. Additionally, this results in a high level of structural vibration. The propulsion system design must be modified to improve the vibration behavior of the ship.

Keywords: Torsional vibration, Structural vibration, Hybrid propulsion system, Composite boat, Electromagnetic clutch

1. Introduction

Eco-friendly ships are key tools in marine industry. Alternative fuels have been used and advanced technologies have been developed and applied to improve their power performance **[1][2]**. Composite materials provide a higher strength-to-weight ratio than traditional materials, such as steel or wood. They enable the construction of a one-piece boat using precision-engineered molds. This results in a greater structural integrity and resistance to stress. It is also easier to process a hull with a lower level of skill. Composite boats are generally easier and more cost-effective to maintain. They are highly resistant to corrosion and water absorption, making them more durable than metals. Another very attractive aspect is that composite boats tend to surf smoothly and are softer and quieter. This improves the comfort of passengers. Lightness, strength, durability, and ease of manufacture make composites increasingly important in the marine industry **[3]-[6]**.

Owing to its lightness, more facilities could be installed on a small boat. By installing an electric motor powered by batteries, the propulsion system can be driven by a diesel engine, an electric motor, or both. This allows the prime movers to alternate, improving flexibility under various maneuvering conditions. The batteries supplying power to the electric motor can be charged in advance by a land-based electric source before boarding or by the electric motor itself in the generator mode. The hybrid propulsion system can offer fuel savings and longer boarding times, and is much quieter in the motor mode **[7]-[12]**. This helps to harmonize economic benefits and environmental protection.

Composite materials and hybrid propulsion systems offer many advantages; therefore, they have been widely applied in the marine industry, especially in small yachts and boats. However, applying new materials and configurations to a ship changes its vibration characteristics. This study focused on a G/T 3-ton class composite fishing boat equipped with a hybrid propulsion system. The general arrangement of the subject boat is depicted in **Figure 1,** and its principal particulars are listed in **Table 1**. The hybrid propulsion pairs a 199 kW Hyundai Seasall diesel engine with a 25 kW electric motor from LG marines (LGM). The specifications of the propulsion system are listed in **Table 2** and the assembly is shown in **Figure 2**.

† Corresponding Author (ORCID: http://orcid.org/0000-0002-6101-7389): Professor, Division of Marine System Engineering, Korea Maritime & Ocean University, 727, Taejong-ro, Yeongdo-gu, Busan 49112, Korea, E-mail: woongsengine@kmou.ac.kr, Tel: 051-410-4571

1 Ph. D., Division of Marine System Engineering, Korea Maritime & Ocean University, E-mail: quangdao.mtb@gmail.com

2 M. S., Division of Marine Information Technology, Korea Maritime & Ocean University, E-mail: top380@g.kmou.ac.kr

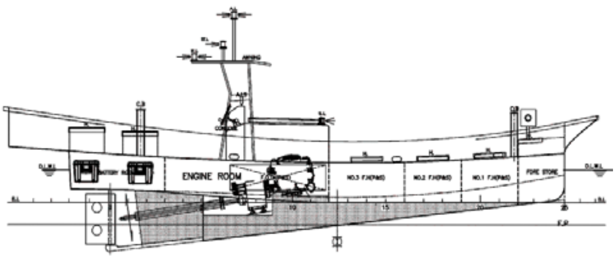

Figure 1: General arrangement of a G/T 3-ton class composite fishing boat

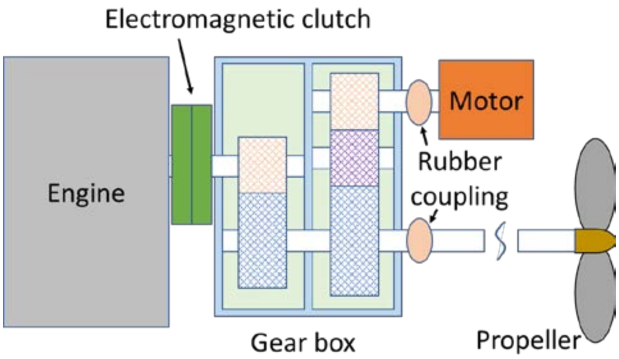

Figure 2: Combined diesel engine and electric motor propulsion system

Table 1: Particulars of the case study ship

Item	Value
Length (O.A)	13 m
Length (B.P)	9.4 m
Breadth (MLD)	2.64 m
Depth (MLD)	0.79 m
Draft (MLD)	0.68 m

Table 2: Specifications of propulsion system

Engine	
Engine type	S270P
Number of strokes	4
Output PS (kW)	270PS (199)
Rpm at full load	3800
Cylinders	V-6
Ignition sequence	1-2-3-4-5-6
Displacement [cm^3]	2959
Bore [mm]	84
Stroke [mm]	89
Compression ratio	17.3±0.5 : 1
Max. torque [kgm] @ speed [rpm]	57.6 @ 2500 51.0 @ 3800
Weight [kg]	327
Gear ratio	6.425 : 1
Motor	
Motor type	LGM-45
Output [kW]	25
Max speed [rpm]	3500
Gear box	
Weight	About 200 kg
Gear ratio in Engine mode	6.425 : 1
Gear ratio in Motor mode	11.760 : 1
Propeller	
Number of blades	3
Weight (ton)	0.0524

An electromagnetic clutch was fitted between the engine and gearbox to engage and disengage the power transmission. It transmits power from the engine during the engine operating mode and cuts off power during the motor operating mode. In the engine operating mode, the torque transmission mechanism equipped with an electromagnetic clutch is more complicated than a clutchless transmission in motor mode. This may lead to a larger torsional vibration in the engine mode. In addition, in the engine operating mode, owing to the combined excitation force of the engine and propeller, torsional fluctuation is much larger than the fluctuation in the rotor mode. A greater torsional vibration on the propeller shaft results in lower propeller efficiency. Thus, the propeller performance was not maximized. Torsional vibration can also cause the electromagnetic clutch to slip internally, which could potentially damage it **[13][14]**. In addition, torsional vibration on the propulsion system leads to an increase in the bearing loads, which also affects the structural vibrations and hull vibrations **[15]-[18]**. It is necessary to comprehensively survey and evaluate the vibrational characteristics of the propulsion system as well as the ship. For this purpose, a series of experiments were carried out during a sea trial to examine the noise and vibration behavior of the hybrid propulsion system in detail.

2. Experimental setup

The setup of the measurement in this study is shown in the schematic in **Figure 3**.

Accordingly, a tachometer-type Compact A2103/LSR/001 was installed at the shaft after the reduction gear to measure the propeller speed. A full-bridge strain gauge type CEA-06-250US-350 of Micro-Measurements was attached to the propeller shaft, as shown in **Figure 4** to achieve torsional vibrations as well as shaft power.

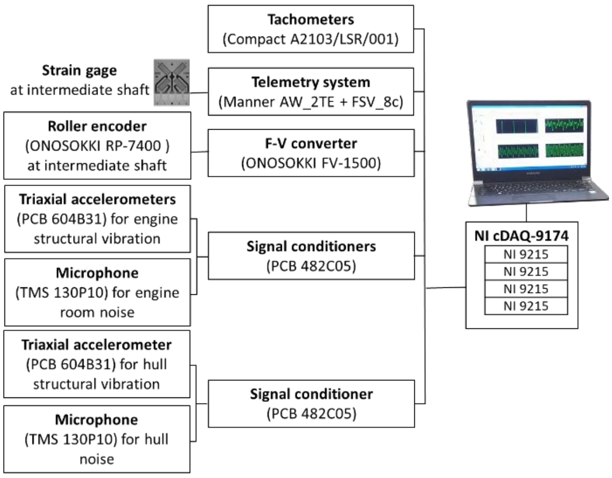

Figure 3: Schematic of the measurement setup

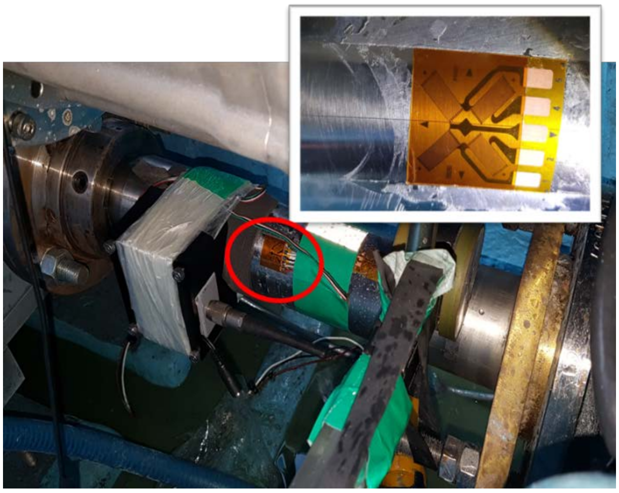

Figure 4: Strain gauge and telemetry system installation at the propeller shaft for torsional vibration measurement

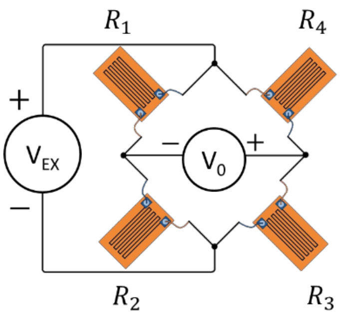

Figure 5: Wheatstone full-bridge of strain gauge configuration

There were four active arms on the strain gauge, and they were configured to form a Wheatstone full bridge, as depicted in **Figure 5**. Each arm was positioned at an angle of 45° to the shaft axis. The torsion strain experienced by the shaft surface was transferred directly to the strain gauge, which responded to a linear change in the resistance of each arm. The output voltage of the Wheatstone bridge circuit measured minute changes in the resistance corresponding to the strain. The sensor signal amplifier (signal transmitter) model was FSV_8c, and the evaluation unit (signal receiver) model was AW_2TE. Both are of the MANNER Sensortelemetrie type with a zero-point drift (accuracy) of less than 0.02%/ °C. The sensitivity was 0.05 to 20 mV/V for a bandwidth of 0 to 1000 Hz.

To measure the shaft rotating angular velocity, an anti-slip roller encoder (type RP-7400, ONO SOKKI) was installed at the propeller shaft, as shown in **Figure 6**. The velocity measurement could be performed at 0.01 m/min (1200 pulses/revolution). A high-speed frequency-to-voltage converter (FV-1500, ONO SOKKI) was used to convert the frequency signal that was proportional to the rotation speed into a voltage signal. It had a high-speed response of 1 cycle + 3.5 μs.

Figure 6: Roller encoder installation at propeller shaft for angular velocity measurement

The installations for the structural vibration and noise measurements are shown in **Figure 7** and **Figure 8**.

Triaxial accelerometers type 604B31 were installed on the engine body and hull deck. The nonlinearity of the accelerometer was less than 1% in the frequency range of 0.5 to 5000 Hz. A 1/4-inch microphone-type TMS 130P10 was installed in the engine room and hull deck for noise measurement. The accuracy of the microphone was ± 2 dB in the frequency range of 10–20,000 Hz.

Type 402C05 signal conditioners provided a current source to the accelerometers and microphones, picked up the signals from the sensors, and converted them to voltage. All the accelerometers, microphones, and signal conditioners were produced by PCB Piezotronics.

(a)

(b)

Figure 7: Triaxial accelerometers installation for the structural vibration measurement. (a) Hull deck; (b) S270P-V6 diesel engine

(a)

and (b).

Figure 8: Microphones installation for noise measurement. (a) Hull deck; (b) Engine room.

3. Results and discussion

3.1 Torsional vibration measurement

Transient torsional vibration is very important when considering the stability, comfortable performance, and full life cycle of a propulsion system as a whole. During the start-up process, clutch engagement may generate a judder phenomenon **[19]-[21]**. This prevents the propulsion system from starting smoothly and could even can damage the transmission system. A clutch engagement-disengagement test was performed to confirm the transient load on the magnetic clutch during these operations. Consequently, dominant self-excited vibrations can occur during engagement [22][23]. The testing procedure is as follows.

Step 1: Start the engine and run it stably at an engine-speed of 700 rpm.

Step 2: Engage the clutch.

Step 3: Keep the engine running stably at a speed of 700 rpm.

Step 4: Disengage the clutch.

The results of torsional vibration measurements at the propeller shaft are shown in **Figure 9** and **Figure 10**. During engagement, the judder phenomenon occurred, but the torque fluctuation was not significant compared with the torque transmitted, as depicted in **Figure 9**. The vibration behavior was much smoother during clutch disengagement, as shown in **Figure 10**. The measured torsional vibration stresses indicated that the clutch worked well during the engagement and disengagement processes.

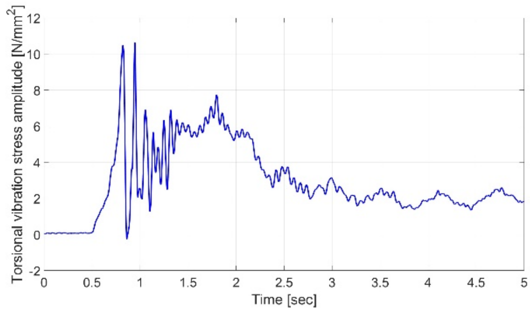

Figure 9: Torsional vibration stress during clutch engagement

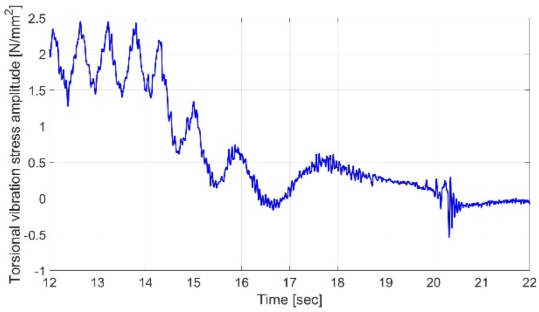

Figure 10: Torsional vibration stress during clutch disengagement

Steady-state measurements under normal operating conditions were also performed to evaluate the vibration characteristics of the propulsion system over the full range of operating speeds. For these measurements, only the engine mode was used. Consequently, after engagement, the propeller speed increased with a slow and steady acceleration from the minimum speed to the nominal speed. The sweep was sufficiently slow to enable the full development of the vibration quantities to be measured. The vibration measurement was in accordance with the ISO 20283-4:2012 standard **[24]** concerning the measurement and evaluation of the vibration of ship propulsion machinery. Accordingly, the sweep took approximately 10 min to complete, to ensure an acceleration rate of less than 15% of the nominal speed per minute. For the best frequency analysis and harmonic order tracking, a sampling rate of 8192 samples/s was applied for the measurement. Harmonic order was defined as a term that relates to the number of events per shaft revolution. This can be obtained as follows:

$$\text{Harmonic order number} = \frac{\text{Vibration frequency}}{\text{Shaft rotational frequency}} \tag{1}$$

A fast Fourier transform (FFT) was performed with a 25600 spectral line resolution, flat top window, and 4096 Hz frequency range. The torsional vibration characteristic can be assessed through dynamic stress measurements using a strain gauge or angular velocity measurement by an encoder. **Figure 11** shows the analysis results of the torsional vibration stress measured at the propeller shaft. A vertical color bar to the right of the axis describes the color scale of the stress amplitude. Accordingly, vibration resonance occurred in the propeller speed range of 300-350 rpm at the 3rd harmonic order. This vibration was caused by the propeller that has three blades. A closer look at the contour map in **Figure 11(b)** shows that the natural frequency of the vibration appears in the range of 15 to 16 Hz. When the 3rd order vibration met the natural frequency, resonance occurred.

The same resonance phenomenon was recorded in the result of the angular velocity analysis at the propeller shaft, as shown in **Figure 12**. The fluctuation of the angular velocity at resonance was very large owing to the 3rd order excitation from the propeller blades. This must be confirmed by the clutch manufacturer, considering the safety of the transmission system. The level of torsional vibration resonance was not sufficiently high to damage the shaft, but it could cause the electromagnetic clutch to slip and become damaged. In addition, the power performance was not maximized.

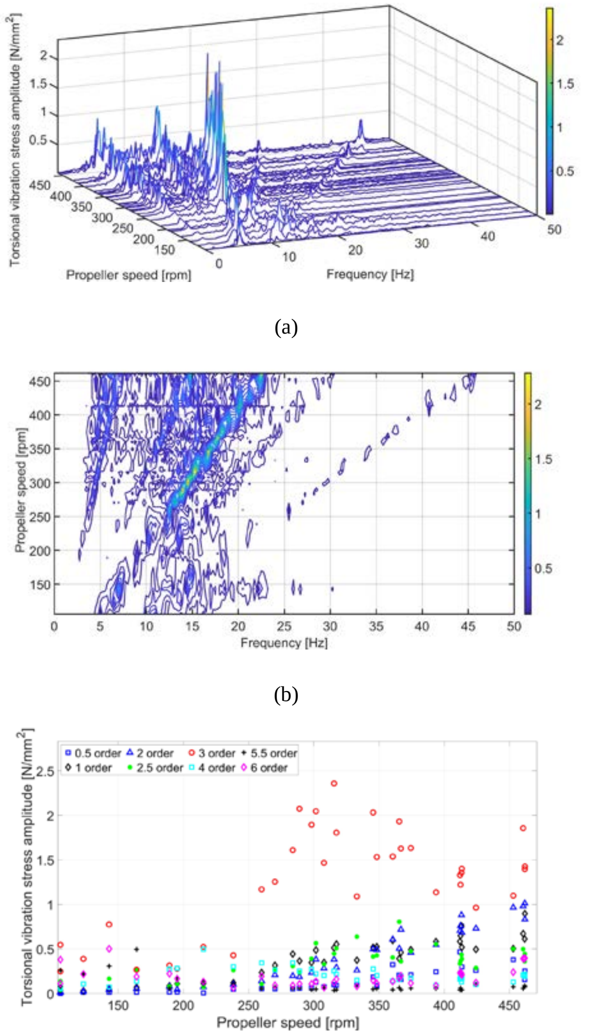

(a)

(b)

(c)

Figure 11: Torsional vibration stress measured at the propeller shaft in engine mode. (a) Waterfall plot; (b) Contour map; (c) All orders plot

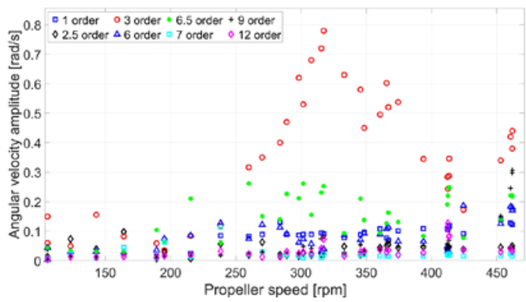

Figure 12: Angular velocity measured at the propeller shaft in the engine mode

3.2 Structural vibration measurement

Structural vibration measurements were performed concurrently with steady-state torsional vibration measurements. A sampling rate of 8192 samples/s was used for the measurement. The sensors were piezoelectric accelerometers that generated acceleration signals. For better evaluation, it is necessary to convert the acceleration data to velocity. For a single-frequency vibration, the velocity vibration in the time domain can be described by

$$v = \hat{v}\cos(\omega t + \varphi_v) \tag{2}$$

Acceleration is the derivative of the velocity with respect to time. The above vibration can be expressed as an acceleration by

$$\begin{aligned} a &= \dot{v} \\ &= -\omega\hat{v}\sin(\omega t + \varphi_v) \\ &= \omega\hat{v}\cos\left(\omega t + \varphi_v + \frac{\pi}{2}\right) \\ &= \hat{a}\cos(\omega t + \varphi_a) \end{aligned} \tag{3}$$

with:

$$\omega = 2\pi f \tag{4}$$

where

- a : acceleration value in the time domain [mm/s^2];
- v : velocity value in the time domain [mm/s];
- $\dot{v}$: derivative of the velocity with respect to time [mm/s^2];
- $\hat{a}$: peak value of acceleration vibration [mm/s^2];
- $\hat{v}$: peak value of velocity vibration [mm/s];
- φ_a: phase of acceleration vibration [rad];
- φ_v: phase of velocity vibration [rad];
- ω : circular frequency [rad/s];
- f : vibration frequency [Hz].
- t : time [second].

From **Equations (2)-(4)** the relationship between the velocity and acceleration at every frequency is established. For the peak value,

$$\hat{v} = \frac{\hat{a}}{2\pi f} \tag{5}$$

For the phase of vibration,

$$\varphi_v = \varphi_a - \frac{\pi}{2} \tag{6}$$

By applying this relationship, we obtained the peak values of the velocity vibration from the acceleration data. First, the acceleration signal in the time domain was processed using an FFT in the same manner as the torsional vibration analysis, as described previously. The data were then converted to a frequency-domain representation that showed the peak value of the acceleration at every vibration frequency. Therefore, the peak values of the velocity vibrations can be obtained using **Equation (5)**. Finally, order tracking analysis was performed based on **Equation (1)** to provide a complete diagnosis of the vibration. **Figure 13** and **Figure 14** show the order tracking results of the structural vibration analysis on the diesel engine body and hull deck near the stern.

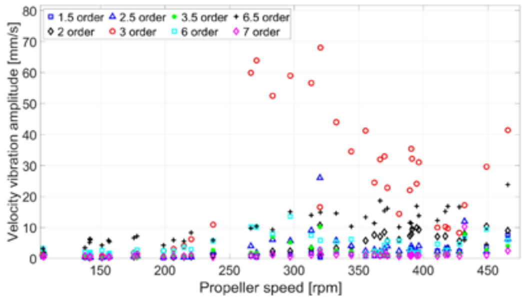

(a)

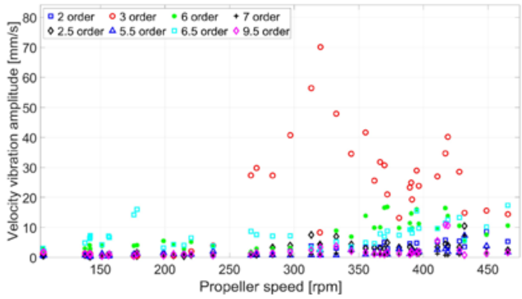

(b)

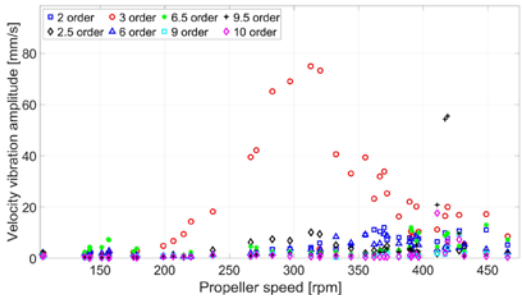

(c)

Figure 13: Structural vibration measured at the top of engine and aft side in engine mode. (a) Longitudinal direction; (b) transverse direction; and (c) vertical direction.

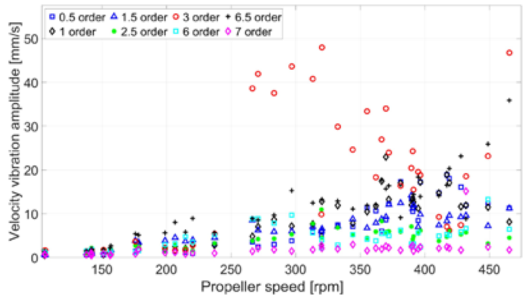

(a)

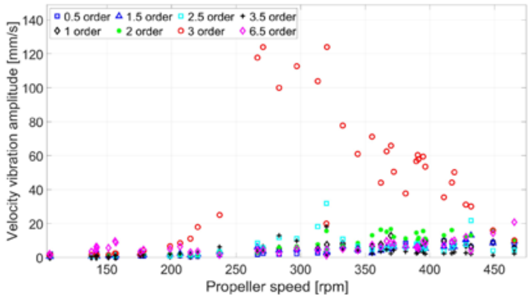

(b)

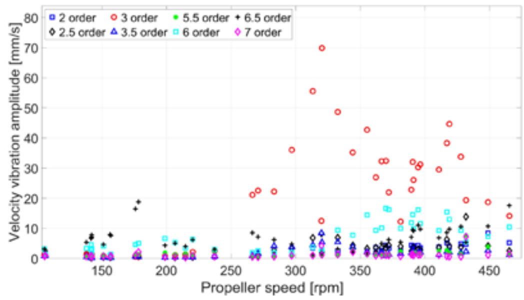

(c)

Figure 14: Structural vibration measured on hull deck near stern. (a) Longitudinal direction; (b) transverse direction; and (c) vertical direction

As a result, vibration resonance occurred at the 3rd harmonic order in the range of 300 to 350 rpm. This phenomenon is similar to the behavior of torsional vibrations. The main excitation source was a 3-blade propeller. The level of the vibration amplitude was much higher than the recommended value of the 30 mm/s peak for the overall vibration amplitude by Lloyd's Register **[25]**. It should be clearly understood that this recommended value applies to steel merchant ships. It may not be applicable to small boats using composite materials. This value was only used for reference. However, it is evident that it affects the human experience on board. Equipment installed on the board is highly susceptible to damage owing to strong vibrations.

3.3 Noise measurement

The noise measurement was carried out at full-speed steady-state operation in both engine and motor modes. The overall noise-level results are listed in **Table 3**.

Table 3: Overall noise level measurement result

Unit: dBA

	Engine mode	Motor mode
Engine room	97	75
Hull deck	85	64

Based on the measurement results, the motor mode showed superior noise reduction. The noise level was significantly improved in both the engine and hull decks. The difference in the overall noise levels between the engine and motor modes was greater than 20 dBA. This proves the advantages of the hybrid propulsion system. It was quieter during the motor operation.

3.4 Discussion

The propulsion system transmits torque from the engine to the propeller and obtains the thrust force from the propeller, which affects the hull. Torsional vibrations also lead to increased bearing loads, which then affect the structural vibration. The exciting forces of the engine and propeller are the main causes of torsional vibration. Based on the measurement results, vibration resonance occurred in the propeller speed range of 300 to 350 rpm at the 3rd harmonic order excited by the 3-blade propeller. The same torsional vibration phenomenon was observed in the angular velocity fluctuation at the propeller shaft. The torsional vibration stress amplitudes were not sufficiently high to damage the shaft, but the angular velocity fluctuation was very large. This can lead to internal slippage of the electromagnetic clutch. The clutch, therefore had a high chance of being damaged. This problem must be confirmed by the clutch manufacturer, considering the safety of the propulsion system. Torsional vibration also affects the structural vibration on the engine and hull deck. The vibration level may not damage the boat hull made of composite material, but it can cause damage to the equipment and impairs the onboard human experience.

The vibration resonance was the result of the 3rd order propeller excitation and a natural vibration frequency in the range of 15 to 16 Hz. It is recommended to change the propeller design from three to four or five blades. In the case of a 5-blade propeller, the propeller excitation frequency was of the 5th harmonic order. Using **Equation (1)** and the same natural frequency of 15–16 Hz, the critical propeller speed was determined in the range of 180 to 192 rpm. Therefore, vibration resonance (if still available) occurs at a lower propeller speed, which is far from the usual operating speed range. In addition, this will change the stiffness and the 2nd moment of inertia of the propeller. A ship design engineer can choose appropriate values to lower the natural frequency while maintaining the propeller efficiency. This change improves the torsional vibration behavior and significantly reduces the structural vibration compared to the current state.

4. Conclusion

Hybrid propulsion systems and composite materials offer several advantages. These include light weight, long service life, low maintenance cost, and high flexibility under various maneuvering conditions. However, the application of a new material and configuration changes the vibration behavior. In this study, the vibration characteristics of a hybrid composite boat were thoroughly investigated and evaluated. The conclusions drawn from this study are as follows:

① The torsional judder phenomenon occurs during the clutch engagement process, but the torque fluctuation is not significant compared to the transmitted torque. The disengaging was smooth. The clutch worked well during the engagement and disengagement processes.

② In the steady-state measurement, vibration resonance was observed in the propeller speed range of 300–350 rpm. This occurred at the 3rd harmonic order frequencies owing to excitation by the 3-blade propeller. The natural frequency of vibration was found to be in the range of 15–16 Hz. When the 3rd order vibration met the natural frequency.

③ The torsional vibration stress amplitudes were not remarkable enough to damage the shaft; however, the angular velocity fluctuation was significant. This could cause the electromagnetic clutch to slip internally and have a high possibility of being damaged. The clutch manufacturer should confirm this by considering the safety of the propulsion system.

④ Torsional vibration of the propulsion system affects the structural vibration. The vibration level may not damage the composite material, but it can cause damage to the boat equipment and impairs the onboard human experience.

⑤ It is recommended to change the propeller design from three to four or five blades. This will improve the torsional vibration behavior and significantly reduce the structural vibration compared to the current state.

⑥ The motor mode exhibited superior noise reduction. This proves the advantages of the hybrid propulsion system.

Acknowledgements

This work was supported by the National Research Foundation of Korea(NRF) grant funded by the Korea government(MSIT) (2021R1G1A1008612110).

Following are results of a study on the “Leaders in industry university Cooperation 3.0” Project, supported by the Ministry of Education and National Research Foundation of Korea.

This research was supported by the BB21plus funded by Busan Metropolitan City and Busan Institute for Talent & Lifelong Education (BIT).

Author Contributions

Conceptualization, Q. D. Vuong and J. -W. Lee; Methodology, Q. D. Vuong, Y. Kim; Software, Y. Kim; Validation, Q. D. Vuong and J. -W. Lee; Formal Analysis, Q. D. Vuong, Y. Kim; Investigation, Q. D. Vuong, J. -W. Lee; Resources, Q. D. Vuong, J. -W. Lee; Data Curation, Q. D. Vuong, Y. Kim; Writing—Original Draft Preparation, Q. D. Vuong, Y. Kim; Writing—Review & Editing, J. -W. Lee; Visualization, Q. D. Vuong; Supervision, J. -W. Lee; Project Administration, J. -W. Lee; Funding Acquisition, J. -W. Lee.

References

[1] T. Lee, and H. Nam, “A study on green shipping in major countries: In the view of shipyards, shipping companies, ports, and policies.” The Asian Journal of Shipping and Logistics, vol. 33, no. 4, pp. 253-262, 2017.

[2] K. H. Lai, V. Y. Lun, C. W. Wong, and T. C. E. Cheng, “Green shipping practices in the shipping industry: Conceptualization, adoption, and implications,” Resources, Conservation and Recycling, vol. 55, no. 6, pp. 631-638, 2011.

[3] S. Ahmed and S. A. Chaudhry, Composites for Environmental Engineering, New Jersey, United States: John Wiley & Sons, 2019.

[4] P. Pandit, K. Singha, A. Jadhav, T. N. Gayatri, and U. Dhara, “Applications of composites materials for environmental aspects,” Composites for Environmental Engineering, pp. 33-55, 2019.

[5] N. Thondavada, *et al.*, “Environmental science and engineering applications of polymer and nanocellulose-based nanocomposites,” Composites for Environmental Engineering, pp. 135-178, 2019.

[6] Composite yacht construction - A better way to build boats. https://westportyachts.com/composite-yacht-construction/, Accessed November 01, 2022.

[7] S. Minami, T. Hanada, N. Matsuda, K. Ishizu, J. Nishi, and T. Fujiwara, “Performance of a newly developed plug-in hybrid boat,” Journal of Asian Electric Vehicles, vol. 11, no. 2, pp. 1653-1657, 2013.

[8] M. Koci and J. Kacani, “Yahts Production, Traditional or Composite Materials, Advantages and Disadvantages.” European Journal of Multidisciplinary Studies, vol. 2, no. 5, pp. 462-467, 2017.

[9] J. Han, J. F. Charpentier, and T. Tang, “An energy management system of a fuel cell/battery hybrid boat,” Energies, vol. 7, no. 5, pp. 2799-2820, 2014.

[10] T. Tezdogan, Z. Shenglong, Y. K. Demirel, W. Liu, X. Leping, L. Yuyang, R. E. Kurt, E. B. Djatmiko, and A. Incecik, “An investigation into fishing boat optimisation using a hybrid algorithm,” Ocean Engineering, vol. 167, pp. 204-220, 2018.

[11] M. Rafiei, J. Boudjadar, and M. H. Khooban, “Energy management of a zero-emission ferry boat with a fuel-cell-based hybrid energy system: Feasibility assessment,” IEEE Transactions on Industrial Electronics, vol. 68, no. 2, pp. 1739-1748, 2020.

[12] Z. Zhou, M. B. Camara, and B. Dakyo, “Coordinated power control of variable-speed diesel generators and lithium-battery on a hybrid electric boat,” IEEE Transactions on Vehicular Technology, vol. 66, no. 7, pp. 5775-5784, 2017.

[13] R. Temporelli, M. Boisvert and P. Micheau, “Accurate clutch slip controllers during vehicle steady and acceleration states,” IEEE/ASME Transactions on Mechatronics, vol. 23, no. 5, pp. 2078-2089, 2018.

[14] F. Liu, L. Chen, D. Li, and C. Yin, “Improved clutch slip control for automated transmissions,” Proceedings of the Institution of Mechanical Engineers, Part C: Journal of Mechanical Engineering Science, vol. 232, no. 18, pp. 3181-3199, 2018.

[15] Z. Liu, W. Li, and H. Ouyang, “Structural modifications for torsional vibration control of shafting systems based on torsional receptances,” Shock and Vibration, 2016.

[16] P. L. Jayananthan and C. Shravankumar, “Torsional vibration characteristics of power transmission system,” IOP Conference Series: Materials Science and Engineering, vol. 402, no. 1, p. 012144, 2018.

[17] Z. Chen, S. Nie, T. Li, T. Lai, Q. Huang, and K. Zhang, “Torsional vibration response characteristics and structural optimization of shale gas compressor shaft system,” Proceedings of the Institution of Mechanical Engineers, Part E: Journal of Process Mechanical Engineering, vol. 236, no. 3, pp. 1256-1266, 2022.

[18] S. Ni, Y. Guo, B. Lv, D. Wang, W. Li, and Z. Shuai, “Analysis of torsional vibration effect on the diesel engine block vibration,” Mechanics & Industry, vol. 21, no. 5, p. 522, 2020.

[19] B. He-yun, W. Huang, and L. Feng-xia. “Investigation of engagement characteristics of a multi-disc wet friction clutch,” Tribology International, vol. 159, p. 106940, 2021.

[20] A. Zambon and L. Moro, “Torsional vibration analysis of diesel driven propulsion systems: The case of a polar-class vessel,” Ocean Engineering, vol. 245, p. 110330, 2022.

[21] L. Li, Z. Lu, X. L. Liu, T. Sun, X Jing, and W. B. Shangguan, “Modeling and analysis of friction clutch at a driveline for suppressing car starting judder,” Journal of Sound and Vibration, vol. 424, pp. 335-351, 2018.

[22] C. C. Bostwick and S. Andrew, Self-excited vibrations during engagements of dry friction clutches, Technical Paper 982846, SAE transactions, SAE International, USA, 1998.

[23] K. Xu, J. Zeng, and L. Wei, “An analysis of the self-excited torsional vibration of high-speed train drive system,” Journal of Mechanical Science and Technology, vol. 33, pp. 1149-1158, 2019.

[24] ISO 20283-4:2012, Mechanical vibration - Measurement of vibration on ships - Part 4: Measurement and evaluation of vibration of the ship propulsion machinery, International Organization for Standardization: Geneva, Switzerland, 2012.

[25] P. Filcek, “Ship Vibration and Noise,” Lloyd’s Register Guidance Notes Revision 2.1, 2006.